Fusion Engineering and Design 132 (2018) 13–17

Contents lists available at ScienceDirect

Fusion Engineering and Design

journal homepage: www.elsevier.com/locate/fusengdes

Two-dimensional numerical simulation of tungsten melting in exposure to pulsed electron beam

A.S. Arakcheev[a,b,c,*], D.E. Apushkinskaya[d,e], I.V. Kandaurov[a], A.A. Kasatov[a], V.V. Kurkuchekov[a], G.G. Lazareva[a,f], A.G. Maksimova[b,f], V.A. Popov[a,b], A.V. Snytnikov[f], Yu.A. Trunev[a], A.A. Vasilyev[a,b], L.N. Vyacheslavov[a,b]

[a] Budker Institute of Nuclear Physics SB RAS, Novosibirsk, Russian Federation
[b] Novosibirsk State University, Novosibirsk, Russian Federation
[c] Novosibirsk State Technical University, Novosibirsk, Russian Federation
[d] Saarland University, Saarbrücken, Germany
[e] St Petersburg State University, St. Petersburg, Russian Federation
[f] Institute of Computational Mathematics and Mathematical Geophysics SB RAS, Novosibirsk, Russian Federation

ARTICLE INFO

Keywords:
Numerical simulation
Pulsed heating
Melting

ABSTRACT

Melting of the surface of tungsten exposed to a pulsed electron beam has been simulated numerically. Comparison of the experimentally measured at BETA facility time dependence of the radius of the molten region with the calculated data has shown that the surface cooling caused by evaporation has a significant effect on the temperature distribution and melting of the material at sufficiently high densities of the surface heating power. This result validates the created theoretical model of the tungsten melting and evaporation in exposure to a pulsed electron beam. The studied mechanism of the limitation of the surface temperature is different from the well-studied vapor shielding. The presented model is a step to correct interpretation of the erosion caused by the melt motion and splashing in exposure to the ITER-relevant pulsed heating by electron beam.

1. Introduction

The components of the first wall and the divertor of the experimental fusion reactor ITER are expected to experience heavy heat load during a discharge [1]. The heat flux will consist of a steady-state component resulting from outflow of plasma along the separatrix of the magnetic field and transient pulsed loads in the form of type I ELMs, thermal quenches, etc. The most intense of these pulsed heat loads lead to melting of even as refractory material as tungsten, which will cover the divertor plates. The melting of the surface layer can result in increase in the material transport along the surface and formation of droplets of the material, which are dangerous to the hot plasma [2–4]. The effect of pulsed heat loads on materials was studied on the specialized test facility BETA. The loads were simulated using an electron beam source [5]. The experiments involved irradiation regimes with temperatures exceeded the melting point of tungsten. This facility uses optical diagnostics, which enable study of the surface state dynamics during pulsed heating, as well as of the residual effects of the exposure. The objective of the presented work is to verify the numerical simulation of melting of tungsten under irradiation at the BETA facility. Experimental simulations of pulsed heat load using an electron beam are significantly different from experimental simulations with a plasma flow at parameters typical to simulations of transient processes in fusion reactor. The heating of material is limited by cooling of the surface due to intense evaporation in the former case and by the vapor shielding in the latter case [6,7]. In the case of heating by an electron beam, the surface temperature growth stops if the rate of the energy losses caused by the evaporation becomes comparable with the heating power. In the case of heating by a plasma flow, the surface temperature growth slows down when the depth of the evaporated layer becomes thick enough to attenuate the plasma flow to the surface. The vapor shielding is well-studied [7], while the limitation of surface temperature caused by the cooling by evaporation was not checked experimentally. However, a correct description of the phenomena is necessary for reasonable interpretation of experimental measurements of the erosion resulting from the melt motion and splashing. So, we have to check the current model of numerical simulation by comparing its results with the experimental data. We used the time dependence of the molten region size as the most reliable absolute quantitative results of dynamical measurements. In addition, the fraction of energy absorbed

* Corresponding author at: Budker Institute of Nuclear Physics SB RAS, Novosibirsk, Russian Federation.
E-mail address: a.s.arakcheev@inp.nsk.su (A.S. Arakcheev).

https://doi.org/10.1016/j.fusengdes.2018.05.008
Received 13 March 2018; Received in revised form 26 April 2018; Accepted 2 May 2018

by the material and lost to evaporation was calculated for the numerically simulated conditions. The discussed regime of the surface temperature limitation by the cooling by evaporation assumes a high density of the evaporated gas. So, the magnetic field is likely to have no significant effect on the evaporation and consequently on the heating of material.

2. Numerical simulation of tungsten melting

In the experiments at the BETA facility, samples of rolled tungsten were exposed to an axisymmetric electron beam [8]. The thickness of the layer in which electrons with an energy of 80–90 keV release their energy (~10 μm, calculated using the data from [9]) is much less than the distance of heat propagation during the heating (~100 μm). For this reason, in the numerical simulation we solved the heat equation with surface heating in a cylindrical coordinate system:

$$\begin{cases} (c(T)\rho(T) + L_m\delta(T,\Delta))\frac{\partial T}{\partial t} = \frac{1}{r}\frac{\partial}{\partial r}\left(r\lambda(T)\frac{\partial T}{\partial r}\right) + \frac{\partial}{\partial z}\left(\lambda(T)\frac{\partial T}{\partial z}\right), \\ \frac{\partial T}{\partial z} = \frac{W(t,r)-N(T|_\gamma)}{\lambda(T)} \text{ at } z = 0, \\ (n, \nabla T) = 0 \text{ at other boundaries}, \\ T = T_{in} \text{ at } t = 0, \end{cases} \quad (1)$$

where $T(r, z, t)$ is the temperature, $c(T)$ is the specific heat, $\rho(T)$ is the density, L_m is the enthalpy of the phase transition, $T_m = 3695\ K$ is the melting temperature, $\lambda(T)$ is the thermal conductivity, $W(t, r)$ is the power of the heat flux of the electron beam, $N(T|_\gamma)$ is the power loss caused by evaporation, $T|_\gamma$ is the boundary temperature, n is the normal to the surface, and T_{in} is the initial temperature, which was taken equal to 273 K. The delta function was smoothed for the numerical simulation in the interval $[T_m - \Delta, T_m + \Delta]$, $\Delta = 5K$:

$$\delta(T,\Delta) = \begin{cases} \frac{1}{2\Delta}, & |T - T_m| \le \Delta, \\ 0, & |T - T_m| > \Delta. \end{cases} \quad (2)$$

Fig. 1 presents the measured time dependence of the total power of heating by the electron beam and radial distribution of the heating power density absorbed by the target. In the numerical simulation, we assumed the heating power to be constant and equal to the average value in a period of 87 μs; the distribution of the time-average heating power density over the surface was measured using X-ray visualization [8]. The heat released on the surface propagates into the material depth. A sample has dimensions of 25 mm x 25 mm and a thickness of 4 mm. Since the sample is heated to a depth of several hundred microns in such a short time, the simulation region was a transverse section of the sample, a region of 7 mm × 0.5 mm. Fig. 2 presents a sketch demonstrating the geometry. As for time, the numerical simulation continued until solidification of the melt.

It is more convenient to proceed in non-dimensional variables, for example, as follows:

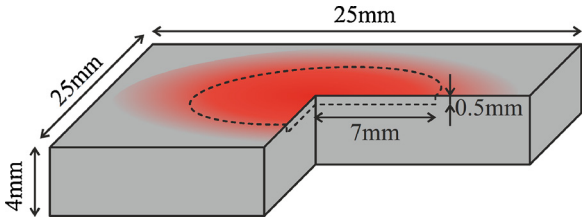

Fig. 2. Sketch of exposed tungsten sample with cut-out quarter, exposed area marked red and dashed line framing region of numerical simulation. (For interpretation of the references to colour in this figure legend, the reader is referred to the web version of this article.)

Table 1
Dimensional parameters of nondimensionalization.

Parameter	Typical value	Units
r_0	10^{-1}	mm
t_0	10^2	μs
λ_0	10^2	$W/mm{\cdot}K$
ρ_0	10^{-5}	kg/mm^3
c_0	10^7	$W{\cdot}\mu s/kg{\cdot}K$
T_0	10^3	K
N_0	10^2	W/mm^2

$$r^* = \frac{r}{r_0}, \quad \lambda^* = \frac{\lambda}{\lambda_0}, \quad \rho^* = \frac{\rho}{\rho_0}, \quad c^* = \frac{c}{c_0}, \quad t^* = \frac{\lambda_0 t}{\rho_0 c_0 r_0^2}, \quad T^* = \frac{T}{T_0}, \quad W^* = \frac{\lambda_0 T_0 W}{r_0}, \quad N^* = \frac{N}{N_0}. \quad (3)$$

The numerical values of the parameters are given in Table 1.

The phase transitions inherent in the problem under consideration are included in the coefficients of Eq. (1). The density (Fig. 3a), thermal conductivity (Fig. 3b), and specific heat (Fig. 3c) are given as dependencies on the temperature of the material in the range $300K \le T \le 8000K$. These functions have discontinuities or lose smoothness at the melting point $T_m = 3695\ K$. The discontinuity of thermal conductivity was smoothed in an interval of 5 K.

Measuring the thermophysical characteristics of refractory metals is a difficult task. Many reference books and articles give approximate or theoretically predicted dependences with an accuracy estimate of 10% and worse. We took the thermal conductivity and heat capacity of solid tungsten from [10], estimates for the thermal conductivity of liquid

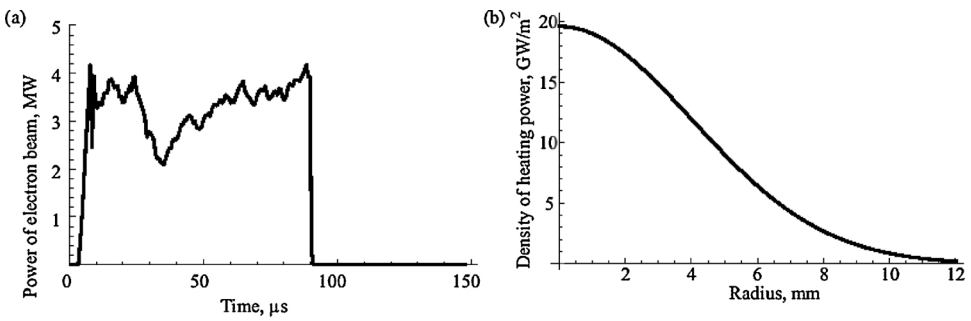

Fig. 1. (a) Time dependence of total beam power and (b) radial distribution of heat flux power absorbed by target.